

Chapter 2

Ferrofluids: A Model System of Self-Organised Equilibrium

Jean-Claude Bacri and Florence Elias

2.1 Introduction: Situation with Regard to the Other Chapters

In this chapter, we shall limit ourselves to studying the morphologies present in an equilibrium state in physical systems: once formed, the structures no longer evolve over time; they remain stable without the need for any further energy to be injected into the system. This means that we can model them by computing the energy balance of the interactions present; the structure obtained and its characteristic length-scale correspond to a minimisation of the system's energy.

We have therefore chosen not to consider dynamic (non-equilibrium) systems, although they can be the site of self-organisation leading to similar periodical patterns. In these dynamic systems, structure formation is generally the result of either dissipative instabilities (such as Rayleigh-Bénard convective instability or Turing instability), or front instabilities (such as Saffman-Taylor instability, or that of Mullins-Sekerka, which leads to the growth of fingers at an interface). Those cases are dealt with in other chapters of the book (see Chaps. 1, 5 and 6).

2.2 Physical Systems in Self-Organised Equilibrium

There is an incredible regularity in the patterns on the coats of leopards, giraffes and zebras. The same patterns can be found throughout the animal kingdom, in seashells, fish, etc. These universal morphologies can be classified according to their elementary design, making up patterns of stripes or spots [1, 5]. Physics also abounds in systems displaying an analogous organisation in equilibrium. They include magnetic films (video and audio tapes), concentrated solutions of surfactants, and many others. These morphologies, in equidistant stripes of equal width or bubbles of the same size spread over a triangular network, can adopt a large-scale architecture and take the form of a labyrinth, for example, or a spiral, a stack of concentric layers

F. Elias (✉)
University of Paris-Diderot, Paris, France
e-mail: florence.elias@univ-paris-diderot.fr

(onions), or intersecting arches (see Chap. 4). Over the course of this chapter, we shall see that although the systems that display such forms of internal architecture are very diverse, and although the nature of the physical parameter used to describe the pattern varies greatly from one system to another, yet the self-organisation itself derives from the simultaneous presence, within a system, of a small number of physical ingredients: a very short-range repulsive interaction, a medium-range attractive interaction and a long-range repulsive interaction are quite sufficient to produce this multitude of equilibrium conformations.

Before abstracting the few physical ingredients necessary to the formation of structures, it is worth analysing the physical systems that display internal morphologies. Figure 2.1 illustrates a number of examples (without claiming to be exhaustive). Below, we shall briefly describe each of these systems and then examine what they have in common and what is specific to each one.

2.2.1 Examples of Self-Organised Physical Systems

2.2.1.1 Magnetic Garnet Films

The first line of the table in Fig. 2.1 presents the example of *magnetic garnet films*. These are thin films made of a material that is ferromagnetic at room temperature. In a ferromagnetic material, the magnetic moments (or spins) of the atoms making up the film tend to align parallel to each other and perpendicular to the plane of the film. This means that the magnetic moments have two possible orientations. When the film is horizontal, these are “upwards” and “downwards”. In the absence of any external magnetic field to break the symmetry of the system in relation to the plane of the film, there are an equal number of magnetic moments in each direction, so that the vector sum of the moments for the whole film is zero. But inverting a spin with regard to its neighbour has an energy cost, because this configuration does not respect the ferromagnetic order. The magnetic garnet film therefore has to minimise the number of pairs of opposite moments. Spins having the same orientation are organised into domains. Domains with opposing magnetisations are separated by walls (known as *Bloch walls*) that contain the energy required to inverse the magnetic moments. The domains themselves are then structured into patterns of monodisperse and equidistant stripes or bubbles. Thanks to the regularity of the bubble pattern, which can be as regular as a perfect crystalline network, information can be stored on magnetic tapes. All it needs is the local application of a magnetic field, to inverse a controlled number of magnetic moments on the film. This creates a defect in the structure, a spatial modulation of the magnetisation, that allows information to be encoded at the desired spot on the magnetic garnet film.

2.2.1.2 Superconductors

A second example of a physical system that self-organises into domains in equilibrium is provided by *type I superconductors*. A superconductor is a material whose electrical resistivity is zero for a temperature T lower than its critical temperature T_c

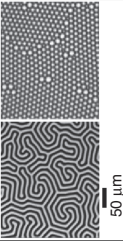
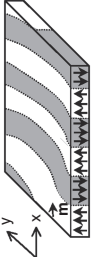
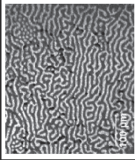
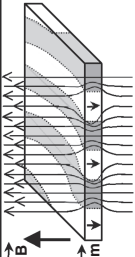



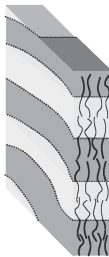
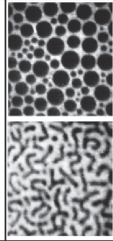

	Bubble and stripes	Sketch	Control parameter	Order parameter	Interactions (SR) short range (MR) middle range (LR) long range
Magnetic garnets			External magnetic field H	Magnetisation $M(x, y) = \sum m_i$	<ul style="list-style-type: none">• Electrostatic interaction (SR)• Boundary energy (attractive, MR)• Energy of dipolar magnetic interaction (repulsive, LR)
Super-conductors			External magnetic field H	Ratio of normal and superconducting phases $\rho(x, y)$	<ul style="list-style-type: none">• Electrostatic interaction (SR)• Interfacial free energy (attractive, MR)• Energy due to the demagnetising field (repulsive, LR)
Pb atoms on Cu			Average Pb surface density $\langle h \rangle$	Rate of Pb surface coverage $h(x, y)$	<ul style="list-style-type: none">• Electrostatic interaction (SR)• Van der Waals energy (attractive, MR)• Elastic energy (repulsive, LR)
Diblock copolymers			Fraction of one component ϕ	Chemical composition $\phi(x, y)$	<ul style="list-style-type: none">• Steric repulsion (SR)• Adhesion (attractive, MR)• Energy of dipolar electric interaction (repulsive, LR)
Langmuir films			Surface pressure π or fraction of one component ϕ	Surface density of molecules $D(x, y)$	<ul style="list-style-type: none">• Steric repulsion (SR)• Line energy (attractive, MR)• Energy of dipolar electric interaction (repulsive, LR)

Fig. 2.1 Examples of morphologies in physical systems. Images: courtesy of P. Molho (magnetic garnets), G. L. Kellogg (Pb atoms on Cu surfaces), H. Jaeger (diblock copolymers) and S. Akamatsu (Langmuir films)

(of the order of between a few degrees Kelvin and a few tens of degrees Kelvin). For a type I superconductor, the phase transition between the normal phase (for $T > T_c$) and the superconducting phase (for $T < T_c$) is of the first order, meaning that there is a range of temperatures below T_c in which domains of superconducting phase coexist with domains of normal phase. The absence of electrical resistivity gives the superconducting phase magnetic properties (diamagnetic, to be more precise). The magnetic field applied is therefore another parameter that, in addition to the temperature, controls the transition between the normal and superconducting phases. When the sample takes the form of a thin film, the application of a magnetic field perpendicular to the plane of the film has the effect of structuring the domains: as in the case of magnetic garnet films, patterns of equidistant stripes or bubbles appear.

2.2.1.3 Lead Atoms on a Copper Surface

Self-organised domains are also formed when a constant flow of lead atoms is deposited on a copper crystal surface, cut along a crystal plane. The interaction between atoms favours the formation of islands of lead on the copper. However, the equilibrium distance between lead atoms is different from the interatomic equilibrium distance of the copper. The interface between the copper and the lead is therefore the site of tensions and compressions, the effect of which is to break up the islands of lead so as to relax the mechanical constraints. These domains are organised into networks of bubbles or stripes separated by about ten nanometres.

2.2.1.4 Diblock Copolymers

Soft matter physics also contains many cases of self-organisation in equilibrium. One example is that of *diblock copolymers*. These are made up of two antagonistic blocks, for example one hydrophobic and the other hydrophilic, joined by a chemical bond. These polymers tend to self-assemble to form a structure aggregating all the blocks with the same affinity, and we can observe the spontaneous appearance of structures whose characteristic thickness is the length of one polymer, about ten nanometres.

2.2.1.5 Langmuir Films

Our last example, also drawn from soft matter physics, is that of *Langmuir films* on the surface of water. These films are composed of molecules of surfactants, which are themselves made up of hydrophilic polar head groups and hydrophobic aliphatic tails. Because of this dual nature, they are also called *amphiphilic molecules*. When they are introduced into water, they tend to adsorb spontaneously to the interfaces, with the heads plunging into the water and the tails pointing out, forming films of monomolecular thickness on the water surface. Depending on the surface density of the amphiphilic molecules present in a Langmuir film, several different phases can be distinguished in these films, analogous to the well-known solid, liquid and gaseous phases in three dimensions. As in the three-dimensional

case, different phases can coexist for certain values of the average surface density of the molecules. It is under these conditions of coexistence that we can observe the presence of domains of one of the two phases within the other. And here, once again, the domains are self-organised into patterns of stripes or bubbles.

2.2.2 The Origin of Order

Why do the same patterns emerge in such different systems? These morphologies are obtained *in equilibrium*: once all the external parameters that can influence the system are fixed, the state of the system no longer evolves. Now, a system in equilibrium is a system that minimises its energy. Our search for the origin of these ordered architectures therefore calls for a careful assessment of all the energy contributions present in the system.

2.2.2.1 Short-Range Repulsion Versus Medium-Range Attraction

A *diphasic system*, that is to say one composed of two immiscible phases, is characterised by the existence of an interface between the two phases. The spatial segregation of the two chemical species present depends on the combined effect of a very short-range repulsive interaction between the molecules of each species (this is usually a hard-core repulsion, preventing the interpenetration of matter and keeping the particles spread out in space) and a longer-range attractive interaction between molecules of the same species. This attraction leads the molecules to aggregate, forming domains of one phase inside the other phase, as a drop of oil does in water (in this case the attractive interaction is the van der Waals force). The standard example of this is van der Waals gas, where the Lennard-Jones interaction energy takes into account these two contributions, allowing to write the gas-to-liquid transition.

However, the creation of boundaries between the two phases has an energy cost (*wall energy*). At the microscopic level, the wall energy derives from the fact that the isotropic attractive interaction between molecules of the same species is not offset near the wall; the molecules situated near the interface are therefore subject to a force that tends to draw them into the domain. At the macroscopic level, the wall energy is minimal when the surface area of the interface separating the two phases is as small as possible. A spherical drop (or circular if the system is two-dimensional) of one phase within the other is the form that minimises the wall energy. In the case of magnetic garnet films, the wall energy is associated with the creation of a Bloch wall; its microscopic origin lies in the ferromagnetic exchange interaction. In the case of islands of lead on a copper surface, the energy cost associated with the creation of walls is connected to interatomic attractions within the solid lead. For systems of diblock copolymers or Langmuir films, the wall energy is due to surface tension (or line tension) of the same nature as that which exists at the interface of a drop of oil in water. Lastly, in the case of type I superconductors, thermodynamic arguments can be used to demonstrate the existence of an interfacial energy between the normal phase and the superconducting phase.

2.2.2.2 Long-Range Repulsion

But why do the systems examined in this chapter form regular structures where the two phases are interlinked with each other? The reason can be found in the existence of a third energy contribution, common to all the systems that possess an internal architecture at equilibrium: an additional *repulsive energy* between the entities that make up the system. In the case of magnetic garnet films and Langmuir films, this repulsive energy is of dipolar origin and acts between two dipoles aligned in the same direction and perpendicular to the plane of the film. At the macroscopic level, this repulsive energy tends to increase the distance between the entities that repel each other, and consequently to increase the surface area of the boundaries. Thus, the formation of stripes or bubbles, or more generally of a multitude of domains of one phase within the other phase, is the result of a compromise between two competing energy contributions: a wall energy that tends to reduce the interface between the two components, and an energy of dipolar origin that tends to lengthen that interface.

However, this competition between two opposing energies does not explain the regularity of the patterns observed. To understand why the domains that emerge all have the same size and are all situated at the same distance from each other, we need one final physical ingredient. These two interactions, one attractive and the other repulsive, do not have the same range of action: the wall interaction, which is attractive, is *medium-range*, whereas the repulsive interaction is *long-range*. In other words, only close neighbours attract each other, while two molecules situated at opposite ends of the system can repel each other. This difference in the range of action naturally introduces a characteristic length scale: the distance between domains. Below this distance, the attractive energy wins out over the repulsive energy and the system tends to form a wall of minimum surface area between the domains. Beyond this characteristic distance, the repulsion is stronger than the attraction, and so the domains tend to become interspersed. We can represent this range difference between the two interactions by the diagram in Fig. 2.2. Imagine that someone is filming the system, while gradually widening the field of vision.

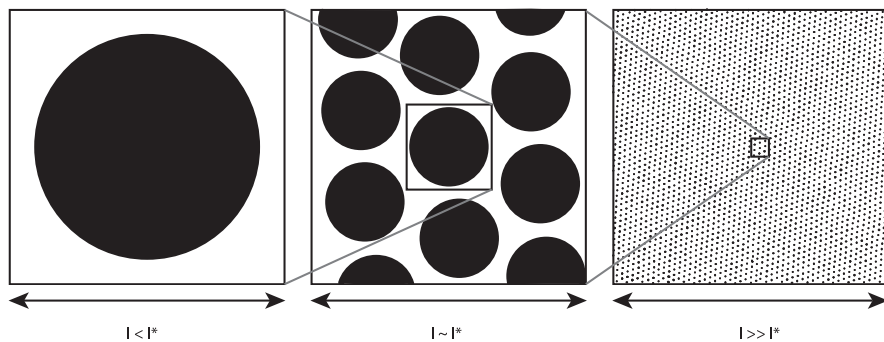


Fig. 2.2 l^* is the characteristic size of the domains, l is the size of the viewing screen through which we observe the system

When the diameter of the display screen is smaller than the characteristic distance between domains, we see one sole domain surrounded by another, which is characteristic of a diphasic system possessing wall energy. Then the field of view widens, and several domains appear, signature of the presence of a repulsive interaction counteracting the wall energy. When the field of view widens still further, we can no longer distinguish the domains: the two phases appear to be dispersed homogeneously throughout the system and the boundaries seem to have disappeared: at large length scales, the effects of the attractive interaction between molecules of the same species can no longer be perceived, only the repulsive interaction appears to be present.

The three ingredients needed to obtain self-organisation of patterns in equilibrium are therefore a very short-range repulsive interaction, a medium-range attractive interaction, and a long-range repulsive interaction. The first two interactions ensure the existence of domains of one phase inside the other, and the third is necessary to the self-organisation of those domains.

2.2.3 The Bond Number

A simple quantitative criterion can be used to determine whether the system under consideration is likely to self-organise. This criterion is provided by dimensional analysis. Based on the two energies that compete to form the patterns, we can define a dimensionless number, the *Bond number*, which is the ratio of repulsive energy to attractive energy. The system self-organises into patterns when the Bond number is greater than 1, whereas it remains divided into two spatially distinct phases when the Bond number is less than 1. The Bond number depends on the external parameter(s) of the system (external magnetic field, total volume or surface area, relative fractions of the two phases, thickness of the system in the case of a quasi two-dimensional system, etc.). We can thus estimate the order of magnitude of the control parameter for which morphologies can emerge.

2.2.4 Domain Size and Choice of Pattern

As the patterns are obtained at equilibrium, we can again make use of energy considerations to calculate the characteristic sizes of the morphologies adopted by the system. These characteristic lengths (the size of domains and the distance between them) are *internal variables*. This means that once the external parameters have been fixed, they adjust in such a way as to minimise the total energy of the system. In practice, therefore, if we write the sum of the two energy terms (repulsive and attractive) according to the internal variable under consideration, and then minimise this energy in relation to the internal variable, we end up obtaining, for example, the domain size as a function of the control parameters.

As several different architectures are possible, we must then perform this operation of minimising the energy in relation to domain size for each pattern (stripes, bubbles or other). We can then insert the equilibrium value of the internal

variable obtained in the expression of the system's energy. The pattern that corresponds to the lowest level of energy is the one that will be chosen at equilibrium – provided that we allow the system the possibility to make this choice, i.e. the possibility to explore all possible morphologies. This point, which is far from evident, will be discussed later in the chapter, using a specific example.

So in theory, knowledge of the two antagonistic interactions at work in the system enables us to draw a phase diagram of possible architectures, and to know all the variables required to describe these structures.

2.2.5 Summary

To sum up, for a system to form regular, structured patterns in equilibrium, a very small number of very general ingredients, common to all systems, is necessary. The characteristic entities of the system must interact through:

- a very short-range repulsive interaction;
- a medium-range attractive interaction;
- a long-range repulsive interaction.

The ratio between the last two energies defines the Bond number, which provides a criterion for the emergence of these internal architectures according to the control parameters of the system. For each system, if we know the expression of these two antagonistic energies, we can establish the phase diagram of possible morphologies and calculate the characteristic size of each structure. This characteristic scale of distance is specific to each system and can vary from a nanometre to a centimetre, depending on the system.

2.3 Morphologies in Ferrofluids

2.3.1 Ferrofluids: A Model System for Studying Structures

Because internal morphologies in the form of stripes or bubbles are universal, and because their existence does not depend on the specific physical properties of the systems that produce them, but on the general form of the energy terms that operate in them, these architectures can be studied through a model system that presents such internal structures. Magnetic liquids, or *ferrofluids*, are one such model system. These liquids combine magnetic properties with ordinary liquid properties (see Box 1). In particular, their interface can change shape under the effect of an external magnetic field [2, 4].

Figure 2.3a shows a few examples of self-organisation where the domains of ferrofluid (in black) form equilibrium structures in a non-magnetic medium: labyrinth, parallel stripes, network of bubbles, foam structure or network of rings [3]. The

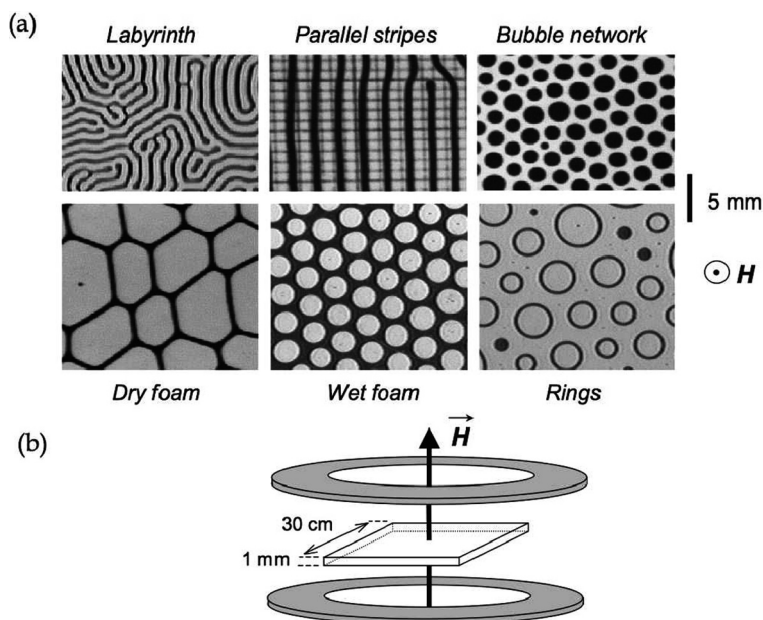


Fig. 2.3 (a) Patterns in 2D ferrofluids: stripes, bubbles, foams and rings. The ferrofluid is in black. The grid that can be seen under the phase in parallel stripes is a millimetre grid. (b) Geometry of the layer of ferrofluid in which the patterns are observed. The cell containing the ferrofluid (*in white*) is placed between two coils of wire (*in grey*) that produce a magnetic field perpendicular to the plane of the cell (a Helmholtz pair)

experimental system used here is two-dimensional: the ferrofluid and a transparent, immiscible, non-magnetic liquid are placed between two transparent plates, about thirty centimetres wide, separated by a spacer one millimetre wide that encloses the cell. The plates are placed horizontally and subjected to a uniform vertical magnetic field of a few hundredths of a Tesla (i.e. a thousand times the magnetic field of the Earth), created using two coils of copper wire in a Helmholtz configuration (Fig. 2.3b). The coils are supplied with an electric current whose intensity can be varied, thus controlling the amplitude of the magnetic field created (which is proportional to the intensity).

From an experimental point of view, there are two main reasons why this sort of layer of ferrofluid makes a suitable model system for the study of self-organised systems. Firstly, these systems are easy to manipulate. Ferrofluids, which behave like ordinary liquids in the absence of an external magnetic field, become magnetic and form structures under the effect of magnetic fields. The choice of structure depends on the amplitude of the field applied. This provides us with a control parameter that can easily be varied in the laboratory, enabling us to sample a multitude of possible morphologies. Secondly, the domain size of most self-organised systems is of the order of micrometres or nanometres, but in the case of ferrofluids it is of the order

of millimetres or centimetres. Observations can therefore be made with the naked eye, avoiding the need for heavy and expensive machines.

In conclusion, the morphologies of ferrofluids are representative of the architectures observed in all self-organised systems. Easy to observe and malleable in the laboratory, they provide us with useful experimental models for understanding self-organised systems.

Box 2.1 Ferrofluids

A ferrofluid is a suspension of solid, magnetic particles in a carrier fluid. These particles are made for example of cobalt ferrite (FeCo) or maghemite ($\gamma\text{-Fe}_2\text{O}_3$). They each carry a permanent magnetic moment, and so they behave like nano-magnets (Fig. 2.4). The magnetic particles have an average size of the order of about ten nanometres. Although they are denser than the water they swim in, this small size allows them to remain in suspension, rather than sinking to the bottom of the container as sediment, because collisions against the molecules of solvent coming from all directions keep them in suspension (Brownian motion). Such homogeneous suspensions of solid particles are called *colloidal suspensions* or *colloids* (this is the case, for example, for India ink, certain paints, and milk). So here, we are dealing with a *magnetic colloid* [2, 4].

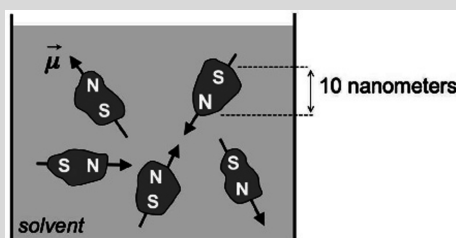


Fig. 2.4 Composition of a ferrofluid. Each particle carries a permanent magnetic moment μ , and so behaves like a miniature magnet, with a North pole and a South pole

Ferrofluids do not exist in a natural state. They are synthesised chemically in the laboratory. To make a stable suspension, it is also necessary to prevent the particles from being attracted to each other by the van der Waals force or magnetic interactions, which would result in the formation of aggregates that would sink under the influence of gravity. Two techniques can be used to achieve this, both consisting in adding a repulsive force between the particles. The first technique produces *surfacted ferrofluids*: the solid particles are covered in surface active molecules (or surfactants), the heads of which adsorb to the surface of the particles. The particles end up covered in a layer of surfactant, which acts like a sort of elastic mattress, maintaining the particles at a

minimum distance from each other, a distance at which the attraction between particles is negligible. The second technique consists in introducing an electrostatic charge of the same sign on the surface of each particle. It is then the electrostatic repulsion between particles that keeps them at a certain distance from each other. To keep the solution electroneutral, counterions (ions of the opposite charge) are introduced into the solution. These counterions have the effect of screening the electrostatic repulsion between the particles, allowing to increase or decrease the distance between particles by decreasing or increasing the concentration of counterions (within the limits of stability of the suspension). This is called an *ionic ferrofluid*. The latter technique makes it possible to use a polar solvent like water, while surfacted ferrofluids are stable in organic solvents like oil.

At the macroscopic scale, in other words at our scale, a ferrofluid is a homogeneous fluid that the magnetic particles have turned black. When a magnet is brought near, the whole liquid is attracted to it. The response of the ferrofluid to a magnetic field is paramagnetic. Let us explain that in more detail. The magnetisation \mathbf{M} of the ferrofluid is given by the vector sum of the individual vector moments of the particles μ_i :

$$\mathbf{M} = \frac{1}{\mu_0 V} \sum_i \mu_i$$

where μ_0 is the vacuum permeability, V is the volume of ferrofluid under consideration and the sum includes all the magnetic particles contained in the volume V . Thus, with a zero field, the magnetic moments are oriented at random because of Brownian motion, and the magnetisation of the ferrofluid is zero. When the amplitude H of the magnetic field \mathbf{H} increases, the magnetic dipoles gradually align in the direction of the field, while the energy of thermal agitation tends to re-establish the disorder. M therefore increases with H . When the field is sufficiently strong, the energy of thermal agitation is defeated by the magnetic energy: all the magnetic dipoles are aligned in the direction of the applied field, and the magnetisation of the ferrofluid saturates at its maximum value. The macroscopic magnetic response of the ferrofluid to a magnetic field is therefore paramagnetic (Fig. 2.5): it is characterised by magnetic susceptibility at zero field:

$$\chi = \lim_{H \rightarrow 0} \left(\frac{dM}{dH} \right) = \lim_{H \rightarrow 0} \left(\frac{M}{H} \right)$$

and by saturation magnetisation M_s . When the volume concentration of magnetic particles is of the order of 10%, $M_s \approx 40 \text{ kA.m}^{-1}$ is reached for an applied magnetic field of the order of 80 kA.m^{-1} (equivalent to a magnetic flux intensity of the order of 0.1 Tesla), and $\chi \approx 1$, which is about one

thousand times higher than the magnetic susceptibility of ordinary paramagnetic liquids. Hence the use of the term “*giant paramagnetism*” to describe the macroscopic magnetic behaviour of ferrofluids.

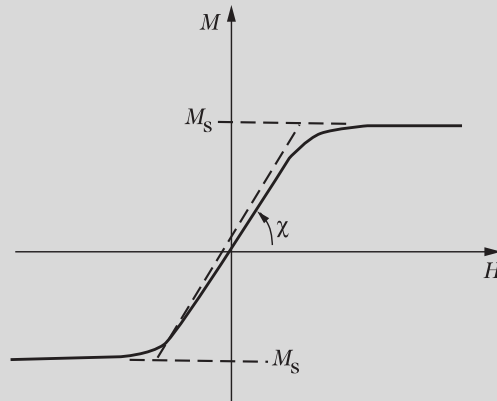


Fig. 2.5 Magnetisation curve of a ferrofluid

2.3.2 *Stripes and Bubbles, Foams and Rings in Ferrofluids*

The equilibrium patterns that emerge in a thin layer of ferrofluid also originate in a competition between short-range repulsive energy, medium-range attractive energy and long-range repulsive energy. The two phases present are a magnetic liquid and another immiscible liquid. In the absence of an external magnetic field, these two phases behave as ordinary liquids. The energies responsible for phase separation are: firstly, the Coulombian repulsion between charged colloidal particles, which plays the role of short-range repulsive energy in the case of an ionic ferrofluid (in surfacted ferrofluids, this repulsion is of steric origin), and secondly, the van der Waals interactions between the molecules of each liquid. Van der Waals forces are always attractive. Their amplitude decreases as the distance between molecules increases, but their range of action is longer than that of the short-range repulsive forces described above, and shorter than the long-range repulsive forces that we shall describe below. The van der Waals interaction is therefore a medium-range attractive interaction.

At the macroscopic level, the van der Waals interaction manifests itself in the form of interfacial tension, which tends to minimise the surface area of the domains. The surface energy is written as: $E_s = \sigma S$, where σ is the surface tension of the interface and S is the total surface area of the interface. In the case of a thin layer of ferrofluid of thickness h (here, $h = 1$ mm), we can write the surface energy as:

$$E_s = \sigma h L , \quad (2.1)$$

where L is the total length of the line separating the two domains. In the absence of an external magnetic field, this attractive interaction is not counterbalanced, which results in the whole system only having two domains, separated by a circular boundary.

2.3.2.1 A long-Range Repulsive Energy

The structuring of the two phases, one within the other, occurs when a magnetic field is applied perpendicular to the layer of ferrofluid. The long-range repulsive energy that opposes the interfacial energy derives from the interaction between magnetic dipoles inside the ferrofluid. This interaction can be explained as follows. The permanent magnetic moments carried by the ferrofluid particles tend to align themselves in the direction imposed by the external field, in the same way as a compass aligns itself in the direction of the magnetic field of the Earth. Now, if you take two permanent magnets, holding them firmly so that their magnetic moments both point in the same direction throughout the experiment, and move them around each other, you will find that when one is above the other they attract each other (their relative position is parallel to the direction of the magnetic moment), whereas when they are side by side they repel each other (their relative position is perpendicular to the magnetic moment). In the case of a layer of ferrofluid subjected to a perpendicular magnetic field, the number of magnetic moments placed side by side is far greater than the number placed above each other. Consequently, the dipoles repel each other, on average. The intensity of the forces of magnetic dipolar interaction decreases as the distance between particles increases, but this decrease is very slow, much slower than the decrease in the intensity of the van der Waals forces: magnetic dipolar interactions are long-range repulsive interactions. The magnetic energy of the layer of ferrofluid is expressed, for a weak magnetic field (see Box 2.2):

$$E_m = - \frac{\mu_0 \chi H_0^2}{2} \int_V \frac{1}{[1 + \chi D(\mathbf{r})]} d^3 \mathbf{r} \quad (2.2)$$

where μ_0 is the magnetic permeability of vacuum, V the volume occupied by the ferrofluid, H_0 the external magnetic field, χ the magnetic susceptibility of the ferrofluid and D the demagnetisation coefficient. Under the hypothesis that the product χD is much less than one, we obtain a simplified expression:

$$E_m = - \frac{\mu_0}{2} \chi H_0^2 V + \frac{\mu_0}{2} \chi^2 H_0^2 \int_V D(\mathbf{r}) d^3 \mathbf{r} . \quad (2.3)$$

The first of the terms on the right-hand side represents the interaction energy between the magnetic dipoles and the field, once the dipoles have aligned themselves in the direction of the field. This term is constant for a fixed value of the external parameters. The second term represents the interaction energy between the

dipoles themselves. It depends on the morphology adopted by the ferrofluid through the factor of demagnetisation and its integral over the volume occupied by the ferrofluid. It is therefore this term that is responsible for the different architectures that the surface of a ferrofluid can adopt.

2.3.2.2 The Magnetic Bond Number and the Characteristic Size of Domains

By expressing the two energy terms whose competition generates the self-organisation, we can define the magnetic Bond number N_B that is characteristic of the system. When the χD tends to zero, it is the ratio of the repulsive energy given by the second term on the right-hand side of the (2.3) over the attractive energy given by (2.1):

$$N_B \approx \frac{\mu_0 \chi^2 H_0^2 V_{FF}}{2\sigma h L} \approx \frac{\mu_0 \chi^2 H_0^2 d}{\sigma} \quad (2.4)$$

where d is the characteristic domain size. Dimensional analysis can be used to estimate the order of magnitude of d by considering that structures emerge when $N_B > 1$: the experimental values of the external parameters ($\chi \approx 1$, $H_0 \approx 10 \text{ kA.m}^{-1}$, $\sigma = 15 \text{ mN.m}^{-1}$) give a value for characteristic domain size of the order of a millimetre, which corresponds well with what we actually observe. However, we can obtain an exact value for the characteristic scales of length (size of domains and distance between them) by expressing the total energy of the system, i.e. the sum of its surface energy given by (2.1) and its magnetic energy given by (2.3), as a function of the internal variables, and minimising the energy in relation to these variables. By performing this operation for all the possible patterns, and then inserting the value obtained for these internal variables into the expression of total energy, we can compare the equilibrium energies of the different morphologies with each other. The most stable equilibrium structure is the one that possesses the lowest level of energy. If several of the structures have the same level of energy, then domains of different morphologies can coexist within the same system.

2.3.3 The Influence of History: Initial Conditions and Conditions of Formation

Calculations show that the numerical value of the energy of a thin layer of ferrofluid differs little from one structure to another. But it requires the injection of a considerable amount of energy, from outside, to make it change from one morphology to another. All the possible patterns that the domains can form are called the *metastable states* of the system: each one corresponds to a local energy minimum, and they are separated by substantial energy barriers. The consequence of this metastability is a strong dependence of the morphology adopted on the initial conditions and the history of the system. To produce a particular morphology, or to change from one

morphology to another, many scenarios are possible, each representing a different recipe for the preparation of the structures.

For example, if the whole ferrofluid is initially aggregated into one sole circular domain when there is zero field, then the pattern formed by increasing the amplitude of the external magnetic field is generally such that the ferrofluid remains connected: we obtain either a labyrinth of stripes of ferrofluid (see Fig. 2.3), or a foam structure. If the most stable state, for a given value of the control parameters (magnetic field, volume fraction of the ferrofluid, thickness of the layer) corresponds to a triangular network of domains in bubbles, then the system must be supplied with sufficient energy to break up the stripes and obtain domains disconnected from each other. We could, for example, wave a small permanent magnet over the layer of ferrofluid, or create cycles in the magnetic field, by rapidly varying its amplitude between zero and the desired value [3]. As the equilibrium period of the patterns is determined by the external parameters, a change in one of those parameters can entail the creation, disappearance or deformation of the domains. In the case of the phase in stripes, disappearance may occur through dismemberment followed by ejection: a stripe breaks in two, and the two halves then creep away from each other. In the case of the foam structure, the domains may coalesce. When a modification of the external parameters imposes a reduction in the period of the structure, the domains may lose their shape and produce new patterns: the bubbles of the triangular phase or the cells of the foam phase may stretch out and take the form of a bean, the stripes may grow fingers or become wavy, the phase in parallel stripes can be periodically deformed to produce a chevron structure. These examples are not exhaustive. In reality, the list of possible patterns grows from day to day: in the laboratory, experimenters regularly discover new, hitherto unobserved forms of organisation within thin layers of ferrofluid, corresponding to new forms of preparation.

Box 2.2 Magnetic Dipolar Interactions and the Magnetic Energy of an Array of Dipoles

At the Microscopic Level

One way to understand magnetic dipolar interactions is to represent the magnetic field \mathbf{H}_m created by a dipole with magnetic moment μ_1 (see Fig. 2.6). The amplitude of the field \mathbf{H}_m decreases spatially as the distance from the moment μ_1 increases. In the plane perpendicular to μ_1 and containing the dipole, \mathbf{H}_m is parallel to μ_1 but oriented in the opposite direction. A second dipole μ_2 placed in this plane therefore feels the effect of \mathbf{H}_m , which tends to align μ_2 in the direction of \mathbf{H}_m . But if the orientation of μ_2 is fixed parallel to that of μ_1 , the dipole cannot turn around. Under these conditions, μ_1 tends to push μ_2 far away, where the influence of \mathbf{H}_m is negligible. On the contrary, \mathbf{H}_m remains oriented in the same direction as μ_1 on a straight line

containing μ_1 and parallel to μ_1 . If a magnetic dipole of moment μ_3 parallel to μ_1 is placed on this straight line, then field \mathbf{H}_m has the effect of reducing the interaction energy between μ_1 and μ_3 . μ_3 therefore tends to move closer to μ_1 to position itself in a field \mathbf{H}_m of even stronger amplitude: the interaction between μ_1 and μ_3 is therefore attractive.

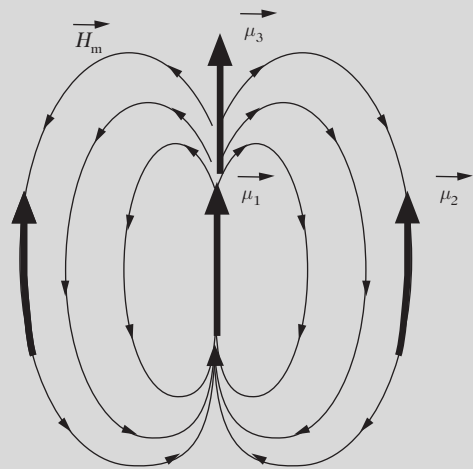


Fig. 2.6 Field lines induced by a magnetic moment

If we assume that the magnetic moments have two possible orientations, upwards or downwards, then we can distinguish four elementary figures (involving two moments) for which the magnetic dipolar interaction is either attractive or repulsive. These four configurations correspond to the different possible orientations of the magnetic dipoles relative to each other. They are represented in the diagram (Fig. 2.7). This description has the advantage of being directly applicable to other physical systems governed by dipolar interactions, magnetic or electrical, like for example magnetic garnet films and Langmuir films.

Attractive dipolar interaction	$\longrightarrow \longrightarrow$ or $\uparrow \downarrow$
Repulsive dipolar interaction	$\longrightarrow \longleftarrow$ or $\uparrow \uparrow$

Fig. 2.7 Four possible instances of magnetic dipolar interaction

At the Macroscopic Level

The magnetic energy of a volume of ferrofluid δV is written as:

$$\delta E_m = -\mu_0 \int_0^{\mathbf{H}_0} \mathbf{M} \cdot d\mathbf{H}_0 \delta V$$

where \mathbf{M} is the magnetisation of the ferrofluid, \mathbf{H}_0 is the external magnetic field and μ_0 the magnetic vacuum permeability. This energy is negative, because that minimises the energy of the system when a magnetic body is placed in a magnetic field; it is all the more negative as the intensity of the field is high. The magnetisation depends on the total magnetic field \mathbf{H} at the point being studied. In a weak field, \mathbf{M} is proportional to \mathbf{H} and the coefficient of proportionality is the magnetic susceptibility: $\mathbf{M} = \chi \mathbf{H}$. The magnetic field \mathbf{H} takes into account the external field \mathbf{H}_0 (which aligns the magnetic dipoles) and the field induced by the dipoles: $\mathbf{H} = \mathbf{H}_0 + \mathbf{H}_d$, where \mathbf{H}_d is the sum, at the point being studied, of the fields \mathbf{H}_m induced by all the dipoles in the ferrofluid (see Fig. 2.6). \mathbf{H}_d is known as the *demagnetisation field*. It is parallel to the magnetisation that gave rise to it, but in the opposite direction: $\mathbf{H}_d = -D\mathbf{M}$, where D is a dimensionless number between 0 and 1, known as the *coefficient of demagnetisation*. Generally, the coefficient of demagnetisation varies spatially through the layer of ferrofluid, but it is homogeneous in a number of simple cases: $D = 1/3$ for a sphere, $D = 0$ for an infinite cylinder subjected to a field parallel to its axis, and $D = 1$ for an infinitely thin plate subjected to a perpendicular field. Given the relations written above, the magnetisation can be expressed in terms of the external field: $\mathbf{M} = \chi \mathbf{H}_0 / (1 + \chi D)$. The magnetic energy of a system containing a volume V of ferrofluid can therefore be written:

$$E_m = -\frac{\mu_0 \chi H_0^2}{2} \int_V \frac{d^3 \mathbf{r}}{1 + \chi D(\mathbf{r})}.$$

The magnetic energy E_m therefore depends on the morphology adopted by the ferrofluid, through the coefficient of demagnetisation D and its integral over the volume occupied by the ferrofluid, which takes into account the effect of magnetic dipolar interactions on the macroscopic level.

2.3.4 The Source of Patterns: Instabilities

An example of the formation of structure can be seen in the first images in Fig. 2.8. The interface of the ferrofluid, which is smooth in zero field (image a), starts to undulate with a well-defined wavelength (image b). Then the crests of the waves grow, forming fingers and then stripes. Between image (a) and image (b), an initially microscopic deformation of the interface has intensified to become visible to the naked eye, in other words macroscopic. This mechanism is due to an *instability* of

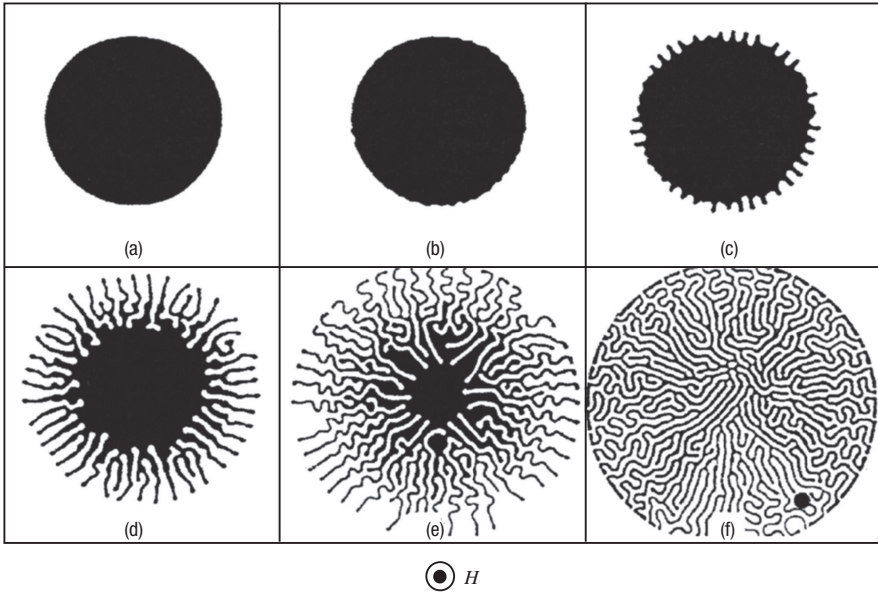


Fig. 2.8 Destabilisation of the interface of a drop of ferrofluid under the effect of a perpendicular magnetic field. (a) Initial situation in zero field. The field is applied from image (b) onwards. The time lapse from image (b) to image (e) is about 3 s. (f) Equilibrium pattern

the interface: the magnetic field exerts pressure on the surface of the ferrofluid, with the effect of amplifying its deformations. Below, we present a number of instabilities of the ferrofluid interface. Normal-field instability (forming spikes) is certainly the most studied and best-known of these instabilities; mathematical processing can be used to discover the value of the amplitude of the magnetic field above which instability occurs, along with the wavelength of the pattern. Lastly, by studying the deformations in a drop of ferrofluid we can bring to light the effects of confinement, which lead to the formation of stripe patterns and bubble patterns.

2.3.4.1 The Showcase of Ferrofluid Instability: Normal-Field Instability

When a ferrofluid is subjected to a homogeneous magnetic field in a direction perpendicular to the liquid-air interface, the surface of the ferrofluid forms a whole series of spikes (see Fig. 2.9a). This spectacular instability occurs when the amplitude of the magnetic field is above a certain threshold value, and the spikes emerge on the surface in a regular network, usually with triangular but sometimes with square symmetry.

Qualitatively, we can explain why this instability appears by considering the different forces present in the case where the surface experiences a weak sinusoidal disturbance. In zero field, the surface of the magnetic liquid, like that of any other liquid, is the site of small, thermally-excited surface disturbances. These are neu-

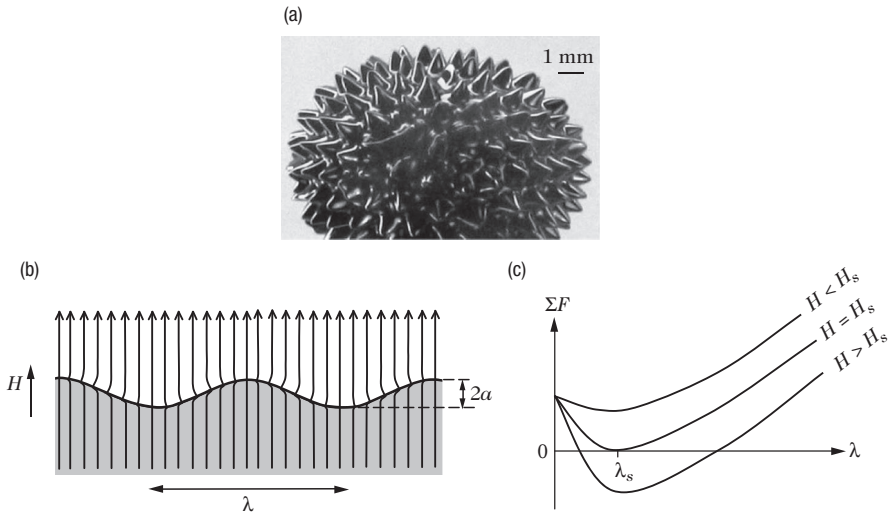


Fig. 2.9 Normal-field instability. (a) The ferrofluid aggregates on the end of a magnet. Its interface forms liquid spikes pointing in the direction of the magnetic field lines. (b) Because of the conditions under which the magnetic field passes through the interface, the magnetic field lines draw together on the crests and spread out in the troughs. (c) Diagram: sum of the forces exerted on a spike as a function of the wavelength of the disturbance, for different values of the amplitude of the magnetic field. The instability can develop on the condition that there exists at least one solution to the equation $\sum F = 0$. There exists, therefore, a threshold amplitude of the field H_s for the development of this instability: the wavelength at the threshold of instability, λ_s , is the capillary length

tralised by the effects of gravitational and capillary forces (linked to the surface tension). When a magnetic field is applied perpendicular to the surface, the field lines draw closer together in the neighbourhood of the wave crests and move further apart from each other in the troughs (see Fig. 2.9b). The field gradients, which are positive in the neighbourhood of the crests, induce a magnetic force (a destabilising force) that tends to amplify the crests and make them more and more pointed. The conformation of the interface results from competition between the forces of gravity and surface tension (stabilising forces) on the one hand, and the magnetic forces, increasing with the amplitude of the field applied, on the other. As long as the amplitude of the field is lower than a certain threshold value, the gravitational and capillary forces win the day, and the interface remains flat. Above the threshold, the magnetic forces are stronger and spikes develop to form a regular network (as in the case of stripe and bubble patterns, this network is linked to the repulsive magnetic interactions between the spikes).

Let us consider the case where the surface of the ferrofluid is the site of a sinusoidal deformation with amplitude a and wavelength λ . We can calculate the threshold amplitude of the field and the wavelength of the instability by means of dimensional analysis, by writing the energy balance of the vertical forces acting on a spike. The spike, comparable to a cone with height $2a$ and diameter λ , has a volume

of $V \approx a\lambda^2$. It is subjected to three vertical forces: the force of gravity F_g , the capillary force F_c and the magnetic force F_m . The amplitude of the force of gravity can be written:

$$F_g \approx \rho g a \lambda^2, \quad (2.5)$$

where ρ is the density of the ferrofluid and g is the acceleration of gravity. The amplitude of the surface force is the derivative of the interfacial energy with respect to a coordinate in the plane of the surface. It is therefore of the order of: $F_s \approx (E'_s - E_s)/\lambda$ where $(E'_s - E_s)$ is the difference between the surface energy with and without spikes. After calculating the surface area of the spike, this gives us:

$$F_s \approx \sigma \lambda (a/\lambda) \approx \sigma a \quad (2.6)$$

where σ is the surface tension of the ferrofluid-air interface. Finally, the magnetic force, resulting from the gradient of the total magnetic field due to the contraction of the field lines crossing the interface, can be written: $F_m \approx -\mu_0 V (\mathbf{M} \cdot \nabla) \mathbf{H}$, that is:

$$F_m \approx -\mu_0 M^2 a \lambda. \quad (2.7)$$

The sum of the forces exerted on the spike can therefore be written:

$$\sum F = F_g + F_m + F_s \approx \rho g a \lambda^2 + \sigma a - \mu_0 M^2 a \lambda \quad (2.8)$$

Fig. 2.9c shows the shape of $\sum F$ as a function of λ for different values of magnetisation. At equilibrium, the sum of these three forces must be zero (fundamental principle of dynamics), and this equilibrium must be stable with regard to a variation in the wavelength of the disturbance:

$$\sum F = 0 \quad \frac{d \sum F}{d\lambda} = 0. \quad (2.9)$$

The equations (2.9) give a system of two equations with two unknowns, the solution of which gives us both the value of the threshold field amplitude H_s and the wavelength λ_s at the threshold of instability:

$$H_s = \frac{M_s}{\chi} = \frac{1}{\chi} \left(\frac{2}{\mu_0} \right)^{1/2} (\sigma \rho g)^{1/4} \quad \lambda_s = \sqrt{\frac{\sigma}{\rho g}} \quad (2.10)$$

where λ_s is the capillary length (the length for which F_g and F_c are of the same order of magnitude).

Another interesting case is that of a thin film of ferrofluid of thickness h , with a magnetic field perpendicular to the interfaces. Experimentally, this is done by depositing a thin film of ferrofluid on the surface of another liquid, but a thin film

suspended by a frame can also be used. The film is said to be thin when its thickness is much less than the capillary length $h \ll (\sigma/\rho g)^{1/2}$. Once again, a weak sinusoidal disturbance is amplified above a threshold field, and then brought back down. Two modes are then possible: the undulation mode (constant thickness) when the two interfaces of the film undulate in phase, and the bulging mode (modulated thickness) when the two disturbances undulate in opposite phase. A similar treatment can be performed by using the equilibrium of forces acting on an elementary volume. In this way, one obtains a diagram of the forces as a function of λ , with the same shape as in the previous example (Fig. 2.9c).

2.3.4.2 The Effect of Confinement in Morphogenesis

All the self-organised systems that we have described up until now have been either two-dimensional (2D) and pseudo-2D systems or patterns created on interfaces. The ferrofluid is also a model system for studying the effects of confinement.

Let us take the example of a drop of ferrofluid with radius R subjected to a magnetic field. When R is much smaller than the capillary length, the forces of gravity are negligible compared to those of the interfacial tension, and the drop is spherical in zero field. When we apply a magnetic field, the drop elongates in the direction of the field (see Fig. 2.10a): this is the effect of the magnetic spike. If we wanted to describe this effect quantitatively, our description would have to be based on the minimisation of the total energy of the system. The total energy of the drop is $E_t = E_s + E_m$ where E_s is the surface energy and E_m is the magnetic energy of the drop. Ellipsoids are magical objects in magnetism (as they are in electrostatics), because the field of demagnetisation is constant inside them. If we accept that a drop of ferrofluid is distorted into an ellipsoid of revolution under the action of a homogeneous magnetic field (which is indeed verified experimentally), then we can calculate exactly the magnetic energy as a function of the stretching of this ellipsoid:

$$E_m = -\frac{\mu_0 \chi V}{2} \frac{H_0^2}{1 + \chi D(a/b)} \quad (2.11)$$

where V is the volume of the drop and a/b is the ratio of the minor axis to the major axis of the ellipsoid. The surface area is also expressed in terms of the ratio a/b . The equilibrium form is given by the minimisation of total energy with regard to the ratio a/b :

$$\frac{dE_t}{d(a/b)} = 0. \quad (2.12)$$

Equation 2.12 produces the curves of Fig. 2.10b, which represents the variation of the ratio a/b as a function of the reduced magnetic Bond number $B_m = \chi H_0^2 R / \sigma$. Note that there is a hysteresis between the rise and fall of the magnetic field.

If we now confine the same drop lengthwise between two planes, a distance h apart from each other, it can no longer stretch in the direction of the field and tries

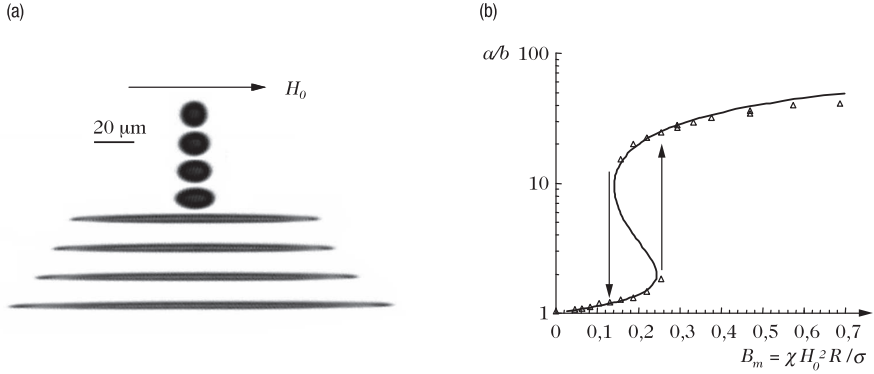


Fig. 2.10 Instability of a drop of ferrofluid subjected to a magnetic field. **(a)** The drop, spherical in zero field, stretches in the direction of the magnetic field applied and takes the form of an ellipsoid of revolution. Beyond a threshold value of the magnetic field, the drop deforms considerably into a needle, pointing in the direction of the field. **(b)** Shape of the drop (ratio of the minor axis to the major axis) as a function of the magnetic Bond number. The *triangles* represent experimental measurements and the *solid line* shows the theoretical curve. For the lower values of the ratio a/b the drop is an ellipsoid; for the higher values it takes the form of a needle. We can see that the ellipsoid-needle instability does not occur at the same value of the magnetic field when the amplitude is increasing and when it is decreasing: there is a hysteresis

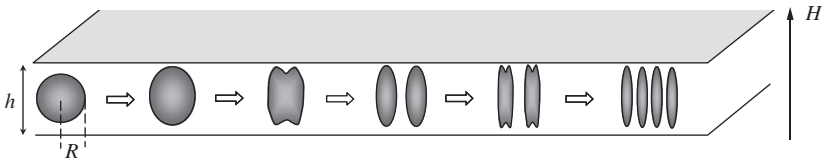


Fig. 2.11 Cascade of splitting in a ferrofluid drop confined between two planes and subjected to a magnetic field perpendicular to the planes, in the case where $R \ll h$. From *left to right*, the amplitude of the field (zero for the spherical drop) increases

to escape in other directions. There are then two possible scenarios, depending on the value of the ratio R/h : if $R/h \ll 1$, the drop separates, in a cascade of splitting (Fig. 2.11). If, on the other hand, $R/h \gg 1$, then fingers emerge on the interface of the drop (see the first images of Fig. 2.8).

In both cases, the appearance of these instabilities can be understood as the loss of stability of an ellipsoid of revolution in favour of an ordinary ellipsoid. But the mathematical treatment is not simple. The ellipsoid model may be appropriate when $R/h \ll 1$, but this is no longer the case when $R/h \gg 1$, because the drop is flattened by the planes confining it. We are then dealing with something more like a cylinder, in which the field of demagnetisation is no longer constant. Calculating the magnetic energy is then a much more complicated task than in the case of an ellipsoid drop.

When $R/h \ll 1$, we obtain a cascade of splitting that results in a network of needles with hexagonal symmetry. The distance between needles decreases as the magnetic field increases: this is the bubble pattern. As Fig. 2.11 illustrates, each division is initiated by a tip-splitting event, with the top of the ellipsoid dividing into two points. Because of the magnetic dipolar repulsion, these two points repel each other, and the splitting process begins. When $R/h \gg 1$, the formation of stripes and the repulsive interactions between stripes leads to the emergence of a labyrinth that occupies the whole space, for a sufficiently high magnetic field (Fig. 2.8). This is because the ribbon form is favourable to the minimisation of magnetic energy: the more intense the magnetic field, the thinner the ribbon.

2.4 Conclusion

We have seen that physics gives us access to a wide diversity of patterns in equilibrium: systems of bubbles, rings, foam, stripes, labyrinths and spikes, and that several ingredients are necessary and sufficient to produce them. Very short-range repulsive interactions and medium-range attractive interactions are needed to obtain a diphasic system with the two phases coexisting in interlinked domains. The equilibrium between medium-range attractive interactions and long-range repulsive interactions leads to the structuring of the domains, with a well-defined characteristic length scale. We have also seen that the effect of confinement can be a necessary condition for self-organisation, because all the systems described are either 2D and pseudo-2D or involve surface effects.

These conditions are satisfied by ferrofluids, where the source of the very short-range repulsion is either Coulombian (charged particles) or steric (surfacted particles), the medium-range attraction is induced by the van der Waals interaction and the long-range repulsion by magnetic dipolar interactions.

All these patterns also appear in the living world, as the photos in Fig. 2.12 show. These are all 2D examples (confined to the surface of the animals. 3D structuring of the interface can also be observed in the animal kingdom (for example the spikes of sea urchins).

We can rediscover some of these patterns by using a model of non-equilibrium instability (Turing instability) in reaction-diffusion systems. Turing instability has therefore become one of the explanations for these patterns (see Chap. 5 by J. Tabony in the present volume). Our conjectures are even simpler. Suppose that there is a mixture of white and black cells in a pseudo-2D system. The very short-range repulsion is caused by steric hindrance. The medium-range attraction leads to the formation of groups of white cells and groups of black cells, entailing that the white-white and black-black attractive interactions are stronger than the white-black or black-white interactions (this effect could be caused by specific adhesive proteins). This interaction will produce islands of black cells in a sea of white cells, but without any particular pattern. Now, if there exist long-range repulsive interactions (for example, a molecule with a long-range repulsive effect on the black cells), the



Fig. 2.12 Organised patterns in the animal kingdom. These morphologies display strong similarities to the equilibrium patterns observed at the interface of ferrofluids. *Stripe patterns*: zebra, tiger. *Bubble patterns*: leopard and hyena. *Foam pattern*: giraffe. ©Digital Stock

islands of black cells will then form similar patterns to those we have just described in self-organised physical systems at equilibrium.

References

1. Andelman D. and Rosensweig R.E. (2009) Modulated phases: review and recent results, *J. Phys. Chem. B* **113**, 3785–3798. Andelman D. (1996) Des zébrures aux motifs à pois, *La Recherche*, February 1996.
2. Bacri J.-C., Perzynski R., and Salin D. (1988) Magnetic Liquids, *Endeavour* **12**, 76. Bacri J.-C., Perzynski R., and Salin D. (1987) Les liquides magnétiques, *La Recherche*, October 1987.

3. Elias F., Flament C., Bacri J.-C., and Neveu S. (1997) Macro-organized patterns in a ferrofluid layer, *J. Phys. I France* **7**, 711–728.
4. Rosensweig R.E. (1985) *Ferrohydrodynamics*, Cambridge University Press (New York).
5. Seul M. and Andelman D. (1995) Domain shapes and patterns: the phenomenology of modulated phases, *Science* **267**, 476–483.

Morphogenesis

Origins of Patterns and Shapes

Bourgine, P.; LESNE, A. (Eds.)

2011, XVII, 346 p., Hardcover

ISBN: 978-3-642-13173-8